Received Date : 02-Feb-2016

Revised Date : 10-Jun-2016

Accepted Date : 10-Jun-2016

Article type : Full length original research paper

The *SCN8A* encephalopathy mutation p.Ile1327Val displays elevated sensitivity to the anticonvulsant phenytoin

Running Title: The response of I1327V to phenytoin

Bryan S. Barker [1, 2], Matteo Ottolini [1], Jacy L. Wagnon [3], Rachel Hollander [3], Miriam H. Meisler [3] and Manoj K. Patel * [1,2].

[1]Department of Anesthesiology and [2]Neuroscience Graduate Program, University of Virginia Health System, Charlottesville, VA 22908 USA, and [3]Department of Human Genetics, University of Michigan, Ann Arbor, MI 48109-5618 USA.

Corresponding author:

Manoj K. Patel, Ph.D., Department of Anesthesiology, University of Virginia Health System, Charlottesville VA, 22908-0710, USA. Tel: +1 434 924 9693 Fax: +1 434 924 2105, (email: mkp5u@virginia.edu).

Key Words: SCN8A, anticonvulsant drugs, sodium channels, epileptic encephalopathy, phenytoin.

Text Pages: 25

Figures: 4

Tables: 2

References: 27

Abstract: 284

Introduction: 480

Discussion: 952

Abstract

Objective: *SCN8A* encephalopathy (EIEE13) is caused by gain-of-function mutations resulting in hyperactivity of the voltage-gated sodium channel $Na_v1.6$. The channel is concentrated at the axon initial segment (AIS) and is involved in establishing neuronal excitability. Clinical features of *SCN8A* encephalopathy include seizure onset between 0-18 months of age, intellectual disability, and developmental delay. Seizures are often refractory to treatment with standard anti-epileptic drugs, and sudden unexpected death in epilepsy (SUDEP) has been reported in approximately 10% of patients. In a recent study, high doses of phenytoin were effective in four patients with *SCN8A* encephalopathy. In view of this observation, we have investigated the relationship between the functional effect of the SCN8A mutation p.Ile1327Val and its response to phenytoin.

Methods: The mutation was introduced into the *Scn8a* cDNA by site-directed mutagenesis. Channel activity was characterized in transfected ND7/23 cells. The effects of phenytoin (100 μM) on mutant and wild type (WT) channels were compared.

Results: Channel activation parameters were shifted in a hyperpolarizing direction in the mutant channel, while inactivation parameters were shifted in a depolarizing direction, increasing Na channel window current. Macroscopic current decay was slowed in I1327V channels, indicating an impairment in the transition from open state to inactivated state. Channel deactivation was also delayed, allowing more channels to remain in the open state. Phenytoin (100 μM) resulted in hyperpolarized activation and inactivation curves as well as greater tonic block and use dependent block of I1327V mutant channels relative to WT.

Significance: *SCN8A* – I1327V is a gain-of-function mutation with altered features that are predicted to increase neuronal excitability and seizure susceptibility. Phenytoin is an effective inhibitor of the mutant channel and may be of use in treating patients with gain-of-function mutations of *SCN8A*.

Key Points:

- The *SCN8A* mutation I1327V was previously identified in two patients with early infantile epileptic encephalopathy (EIEE13).
- Electrophysiology analysis of I1327V demonstrated altered activation and inactivation parameters that are pro-excitatory.
- Deactivation and transition from open state to inactivated state were impaired.
- The effect of the anticonvulsant drug phenytoin on tonic inhibition and use-dependent block was greater on mutant than on wild type channels.
- Phenytoin may be effective in suppressing seizures in some *SCN8A* gain-of-function mutations.

Key Words: SCN8A, anticonvulsant drugs, sodium channels, epileptic encephalopathy, phenytoin.

Introduction

Sodium (Na) channels play a critical role in controlling neuronal excitability since they are directly involved in action potential generation and conduction, and also play a role in the transition between single spiking and bursting in some neurons.[1] Pro-excitatory alterations in Na channel function have been reported in patients with epilepsy,[2,3] and in animal models of epilepsy.[4,5] The Na channel isoform $Na_v1.6$ is encoded by the *SCN8A* gene and is highly localized along the axonal initial segment,[6] the site of action potential generation, and at nodes of Ranvier.[7] In some acquired epilepsy $Na_v1.6$ expression is increased,[4,8] and reducing $Na_v1.6$ has been shown to impair the initiation and development of kindled seizures.[4]

De novo missense mutations of *SCN8A* are associated with early-infantile epileptic encephalopathy (EIEE). Since the discovery of the first mutation,[9] more than 100 additional mutations have been identified and collectively defined as EIEE13.[3] Most patients with EIEE13 have seizure onset between birth and 12 months of age, with a median age of onset of 4 months. After the onset of seizures there is significant developmental regression that results in mild to severe intellectual disability. Sudden unexpected death in epilepsy (SUDEP) has been reported in approximately 10% of patients.

Electrophysiology studies on a limited number of mutations demonstrate that many have a gain-of-function characteristic.[9–11] Interestingly, the mechanism by which this pro-excitatory endpoint is achieved differs amongst the mutations. In some, there is an increase in persistent Na current and pro-excitatory shifts in channel inactivation parameters while in others there is a leftward shift in the voltage dependence of activation. A knock-in mouse model carrying the *SCN8A* mutation p.Asn1768Asp possesses many of the pathological phenotypes seen in human patients, including seizures and sudden death.[12]

Since the seizures in many EIEE13 patients are associated with a gain-of-function in Na channel activity, a rational approach to therapy would be to use anticonvulsants with Na channel blocking characteristics. However, the seizures in

EIEE13 patients are difficult to control even with Na channel blockers and many patients remain refractory. A recent study of four children with EIEE13 demonstrated good seizure control with high doses of phenytoin.[13] One of these patient mutations included in the study has been examined functionally and shown to result in a hyperpolarizing shift in voltage-dependence of activation.[10] In the current study, we determined the biophysical properties of another *SCN8A* mutation, p.Ile1327Val, located within the highly conserved region of transmembrane segment 5 adjacent to the cytosolic interface of the S4-S5 linker of domain III.[14] Our data show that I1327V is a gain-of-function mutation that is predicted to lead to increased neuronal activity and the generation of seizures. We demonstrate that phenytoin (100 μM) results in greater tonic block and use dependent block of I1327V channels compared with WT channels. The preferential effect of phenytoin on the mutant channel may increase the effectiveness of phenytoin in treating refractory seizures associated with EIEE13.

METHODS

Site-directed mutagenesis of the $Na_v1.6$ cDNA.

The amino acid substitution I1327V was introduced into the tetrodotoxin (TTX)-resistant derivative of the full- length $rNa_v1.6$ cDNA clone (NM_014191.3, NP_055006.1),[15] as previously described.[9,10,16] Site-directed mutagenesis was carried out with the QuikChange II XL kit (Agilent Technologies). The entire 6-kb open reading frame was sequenced to confirm the absence of other mutations.

Cell Culture. DRG-neuron derived ND7/23 cells (Sigma Aldrich) were grown in a humidified atmosphere of 5% CO_2 and 95% air at 37ºC in Dulbecco's Modified Eagle Medium (DMEM 1X) supplemented with 10% FBS, NEAA and Sodium Pyruvate. Cells were plated onto petri dishes 48 hours prior to transfection and transfected for 5 hours in non-supplemented DMEM using Lipofectamine 3000 according to manufacturer instructions (Life Technologies) with 5 μg of $Na_v1.6$ alpha subunit cDNA and 0.5 μg of the fluorescent m-Venus bioreporter. Electrophysiological recordings of fluorescent cells were made 48 hours after transfection.

Electrophysiology. Recordings were carried out in the presence of 500 nM tetrodotoxin (TTX) to block endogenous sodium currents in the neuron-derived ND7/23 cells. Currents were recorded using the whole-cell configuration of the patch clamp recording technique as previously described.[16] Currents were amplified and low-pass filtered (2 kHz) and sampled at 33 kHz. The intracellular recording solution contained (in mM): 140 CsF, 2 $MgCl_2$, 1 EGTA, 10 HEPES, 4 Na_2ATP, 0.3 NaGTP (pH adjusted to 7.2 with CsOH, osmolarity adjusted to 300 mosM with sucrose). Cultured ND7/23 cells were bathed in solution containing (in mM): 130 NaCl, 3 KCl, 1 $CaCl_2$, 5 $MgCl_2$, 0.1 $CdCl_2$, 10 HEPES, 30 TEA (pH adjusted to 7.4 with NaOH, osmolarity adjusted to 310 mosM with sucrose). Experiments were performed at room temperature (20-22ºC). After establishing the whole cell configuration, a minimum series resistance compensation of 75% was applied. Capacitive and leak currents were subtracted using the P/4 protocol for all experiments, except steady-state inactivation protocols. The current-voltage relationship was determined using a 100 ms voltage pulse from -80 to +70 mV in steps of 5 mV from a holding potential of -120 mV at 2 sec intervals. Conductance as a function of voltage was derived from the current-voltage relationship and fitted by a Boltzmann function as described.[8] Decays of macroscopic currents were fitted to a single exponential function and time constants were determined. For steady-state inactivation, neurons were held at -120 mV and test potentials from -115 mV to -10 mV for 500 ms at 5 mV increments were applied. The second pulse to -10 mV for 40 ms was used to assess channel availability. Correction for passive and leak currents was achieved by subtracting the last sweep with the greatest depolarizing potential (-10 mV) since this sweep displays no sodium channel current. Currents during the second pulse were normalized for each cell with the largest current as 1.0 and fit to the Boltzmann function. Deactivation was estimated from current decay, using a 0.5 ms short depolarizing pulse to -10 mV followed by a 50 ms repolarizing pulse to potentials ranging from -40 to -120 mV at 5 mV increments. Deactivation kinetics was determined by fitting decaying currents with a single exponential function. For recovery from inactivation, cells were held at -120 mV and depolarized to a test potential of 0 mV for 1 sec to inactivate Na channels. Recovery was determined at times between 1 ms and 60

sec at a test potential of -90 mV. A 40 ms pulse to -10 mV was subsequently applied to assess the extent of channel recovery. For each cell, current amplitudes during the test pulse were normalized so that the largest current during the conditioning potential was 1.0. Data was then fit to a double exponential function as previously described [8].
For experiments involving the testing of phenytoin, electrophysiological protocols under control, drug free conditions were obtained before bath application of phenytoin (100 μM; 10 mins).

Data Analysis

Data represent means ± standard error of the mean (S.E.M). Statistical significance was determined using a Student's t-test or a standard one way ANOVA followed by Tukey's or Dunn's post hoc test for parametric data or the Rank Sum test for non-parametric data (GraphPad Prism 6).

RESULTS

Electrophysiological characterization of I1327V

Isoleucine residue 1327 is located in the highly conserved region of transmembrane segment 5 of domain III (D3S5) adjacent to the cytosolic S4-S5 linker of $Na_v1.6$ (Figure 1A). Representative currents from ND7/23 cells transfected with wildtype (WT) and I1327V $Na_v1.6$ are shown in Figure 1B. Peak current density for I1327V was not elevated compared to WT (Figure 1C). Analysis of steady-state kinetics demonstrates a small but significant hyperpolarizing shift in the half maximal voltage dependence of activation for I1327V ($V_{1/2}$) of -2.5 mV ($p<0.05$: Figure 1D, E). Slope factor (k) was also significantly decreased ($p<0.005$: Figure 1F, Table 1). To determine the kinetics of open state inactivation, macroscopic current decay was fit to single exponential functions and the fast time constant (T) was plotted as a function of voltage. Transition from open state to the inactivated state was significantly delayed in I1327V channels at depolarizing voltages ranging between +15 mV to +35 mV (Figure 1G),

consistent with the prediction of disrupted inactivation. The slowing of fast inactivation is evident when the peaks of the current traces at +35 mV are aligned so that inactivation kinetics can be compared directly (Figure 1H). When examined at a time point of 100 ms after the voltage stimulus, decay of macroscopic current was complete for both I1327V and WT, indicating the absence of increased persistent current in the mutant channel (data not shown).

We next determined the effects of I1327V on the kinetics of channel deactivation. Compared to WT channels, I1327V significantly increased the time constant (T) of deactivation over the range of voltages between -55 mV and -40 mV (Figure 2A), indicating a slower transition from the open state back to the closed state. Disruption in normal inactivation processes have been described for several *SCN8A* mutations.[16] In I1327V channels a significant depolarizing shift in the $V_{1/2}$ of steady-state inactivation was recorded (5.7 mV; $p<0.005$: Figure 2B, C) with no change in slope values (Figure 2D). Window currents can be determined by taking the area under the overlapping normalized activation and inactivation curves (Figure 2E). We determined the window current for I1327V and WT channels and found an increase in the window current for the mutant channel (Figure 2F). Lastly, we examined recovery from inactivation using a recovery voltage of -90 mV and found no significant difference between WT and I1327V transfected cells (Figure 2G; Table 1).

Inhibition of I1327V by phenytoin.

The anti-epileptic drug (AED) phenytoin (Dilantin®) is clinically used to treat epileptic seizures. The mechanism is thought to involve the inhibition of Na channels.[18] Phenytoin binds preferentially to the inactivated form of $Na_v1.6$ and the drug can block high frequency firing of action potentials, trapping channels in the inactivated state.[18] Since I1327V displayed disrupted inactivation parameters we sought to determine if phenytoin would inhibit currents evoked from a holding potential of -60 mV, a potential when many of the channels can cycle between the closed, open and inactivated states. At a concentration of 100 μM, tonic block by phenytoin was significantly greater for I1327V currents (53 ± 2.0%; n=10) than WT currents (43 ± 2.0%; n=8: $p<0.05$; Figure 3A and B). In addition to voltage dependent block, AEDs also exhibit use-dependent

block as an important mechanism of action, permitting enhanced block of high frequency neuronal firing associated with epileptic seizures.[19] In a similar manner to tonic block, phenytoin (100 μM) produced a greater use dependent block of I1327V channels compared to WT (Figure 3C). In the absence of phenytoin, there was very little block of control (6.0 ± 1.0 %; n=23) and I1327V (7.0 ± 1.0 %; n=29) channel currents during the use dependent protocol. In the presence of phenytoin, WT channels were blocked by 11 ± 2.0 % (n=12) at pulse 60. In contrast, phenytoin caused greater use-dependent block of I1327V channels, blocking the current by 21 ± 4.0 % (n=9) ($p<0.05$).

Phenytoin (100 μM) also caused a hyperpolarizing shift in the voltage dependence of activation for both WT channel ($V_{1/2}$ by -7.6 mV; $p<0.05$; Figure 3D-E) and I1327V channels ($V_{1/2}$ by -16.9 mV; $p<0.05$: Figure 3F-G). Phenytoin had no effect on the slope (k) in WT or I327V channels (Table 2). Inactivation parameters were significantly shifted in a hyperpolarized direction by phenytoin (100 μM) for both WT ($V_{1/2}$ by -15.4 mV; $p<0.05$; Figure 4A-C) and I1327V ($V_{1/2}$ by -13.0 mV; $p<0.005$: Figure 4D-F). Slope factors (k) remained unchanged for both WT and I1327V (Table 2). Phenytoin did not significantly alter either the fast or slow time constants of recovery from inactivation at – 90 mV in either I1327V or WT transfected cells (Table 2). Phenytoin did, however, significantly decrease the amplitude of the Na current recorded after a recovery interval of 60 s in WT (47.3% ± 3.4 Figure 4G) and I327V (33.6% ± 11.3 Figure 4H).

DISCUSSION

The *de novo* mutation I1327V was identified in two unrelated patients with early onset encephalopathy.[14,20] Residue Ile1327 is located within the highly conserved region of transmembrane segment D3S5 adjacent to the cytosolic interface with the S4-S5 linker. Mutation studies indicate that residues located along the S4-S5 linker of domain III are critical to fast inactivation since they provide an interaction site for the fast inactivation gate.[21] Since isoleucine and valine are relatively similar in structure and both are non-polar, hydrophobic amino acids, the mechanisms behind disrupted inactivation are not obvious. We hypothesize that substituting the bulky isoleucine side chain with methyl and ethyl groups, for the smaller valine side chain, composed only of

methyl groups, may disrupt the hydrogen bonds that form between the inactivation gate and the S4-S5 linker of domain III, disrupting the normal activation process.

Consistent with the gain-of-function mechanism, I1327V resulted in a hyperpolarizing shift in activation parameters, enabling mutant channels to open at voltages more negative than WT channels. This shift, coupled with a depolarizing shift in the voltage dependence of inactivation, would extend the voltage range where channels would be available for activation and have a finite probability of opening. This range of voltages is commonly referred to as the window current and an enhancement in this current would reduce action potential thresholds, facilitating action potential firing and potentially initiating seizure generation and spread. Increases in window currents have been associated with increased persistent sodium current activity and epileptogenesis in animal models. [22,23] A delay in the decay of the macroscopic current at depolarized voltages further supports the view that a valine for isoleucine substitution at position 1327 results in a major disruption of the normal inactivation process in the mutant channel, specifically delaying entry into the inactivated state. A slowing in channel deactivation would increase the availability of Na channels by delaying the transition of open channels back into the closed state during short depolarizations, further increasing the probability that channels remain in the open state configuration for longer periods of time.

There is considerable heterogeneity among the 10 *SCN8A* mutations that have now been characterized through electrophysiology studies. One common pathogenic mechanism is a disruption in the inactivation process. In some cases, including the current mutation I1327V, this is due to a depolarizing shift in the inactivation curve that delays channel inactivation,[11] while other mutations have normal voltage dependence of inactivation with an increase in persistent Na channel current after prolonged depolarization.[9] Many of these mutations are located at sites involved in channel inactivation, including domain III, IV and the C-terminus.[3] In contrast, two mutations located within transmembrane segments of domain II have normal inactivation parameters, but establish a gain-of-function phenotype via hyperpolarizing activation curves, thereby increasing channel availability at more negative membrane potentials and consequently increasing window currents.[10,11]

AEDs that inhibit Na channels as a mechanism of action have been used in treating seizures in EIEE13 patients. However, it is unclear which AEDs should be considered first choice for these patients. Furthermore, mechanistic studies demonstrating the response of mutant channel currents to AEDs are lacking. In a recent study of four patients with seizures that were refractory to many AEDs, good seizure control was obtained with high dose phenytoin.[13] Withdrawal of phenytoin resulted in seizure reoccurrence in all four patients. This work suggests that phenytoin may be more effective for *SCN8A* encephalopathy than other clinically available AEDs. The mode of action of phenytoin includes inhibition of Na channels, but it also effects calcium channels.[18,24] Phenytoin has little effect on Na channels in their resting or closed state, but at more depolarized potentials, such as those observed during high frequency firing, the block by phenytoin is pronounced.[18,25] This greater affinity for the inactivated state of the channel over the closed state of the channel is an important characteristic of many AEDs.[26] When tested on the mutation I1327V, tonic block and use dependent block by phenytoin was more pronounced for the mutant channel than WT channels. A likely explanation is that phenytoin binds slowly to open and inactivated channels.[18] The mutant channel displayed impaired deactivation kinetics and slowed transition from the open state to the inactivated state at depolarized voltages, allowing channels to remain longer in non-closed conformation. Increased proportion of channels in open and inactivated states would increase the time available for phenytoin to bind tightly and trap the mutant channels in a non-conducting conformation, preventing them from contributing to action potential initiation. This feature is referred to as the modulated receptor hypothesis.[27] Phenytoin also reversed the depolarizing shifts in inactivation recorded with I1327V and caused further hyperpolarizing shifts in activation curves. In view of these findings, patients with the I1327V mutation may achieve good seizure control with phenytoin in a similar manner to the patients reported in the study by Boerma *et al*.[13]

The mutation described here has been observed in two patients to date. The first patient was a male child who experienced seizures immediately after birth and continued to experience refractory epilepsy until his death at the age of 1 year and 5 months.[14] It is unclear whether this patient was treated with phenytoin. The second

patient was a male child who appeared to experience seizures in utero, perceived as "drumming" sensations during the later stages of pregnancy.[20] Although several AEDs were unsuccessful at providing seizure control in this patient, a high dose of phenytoin (18-20 mg/L) did provide temporary seizure control. Both patients had severe, early-onset movement disorders. Our study demonstrates that these patients had a gain-of-function mutation of *SCN8A* which likely accounted for their epileptic encephalopathy. The effectiveness of phenytoin at inhibiting the mutant channel currents provides additional evidence that phenytoin may be a useful treatment for *SCN8A* encephalopathy.

Acknowledgments

We are grateful to Drs. Sulayman Dib-Hajj and Stephen G. Waxman for providing the $Na_v1.6$ cDNA. This work was supported by National Institutes of Health-National Institutes of Neurological Disorders and Stroke grants (NINDS) R01NS075157 (MKP) and RO1NS34509 (MHM). JLW is a recipient of a postdoctoral fellowship from the Dravet Syndrome Foundation.

Disclosure of Conflicts of Interest

None of the authors has any conflict of interest.

Ethical Publication

We confirm that we have read the Journal's position on issues involved in ethical publication and affirm that this report is consistent with those guidelines.

References

1. Cooper DC, Chung S, Spruston N. Output-mode transitions are controlled by prolonged inactivation of sodium channels in pyramidal neurons of subiculum. *PLoS Biol* 2005;3:e175.
2. Vreugdenhil M, Hoogland G, van Veelen CW, et al. Persistent sodium current in

subicular neurons isolated from patients with temporal lobe epilepsy. *Eur J Neurosci* 2004;19:2769–2778.

3. Wagnon JL, Meisler MH. Recurrent and Non-Recurrent Mutations of SCN8A in Epileptic Encephalopathy. *Front Neurol* 2015;6:104.
4. Blumenfeld H, Lampert A, Klein JP, et al. Role of hippocampal sodium channel Nav1.6 in kindling epileptogenesis. *Epilepsia* 2009;50:44–55.
5. Hargus NJ, Merrick EC, Nigam A, et al. Temporal lobe epilepsy induces intrinsic alterations in Na channel gating in layer II medial entorhinal cortex neurons. *Neurobiol Dis* 2011;41:361–376.
6. Hu W, Tian C, Li T, et al. Distinct contributions of Na(v)1.6 and Na(v)1.2 in action potential initiation and backpropagation. *Nat Neurosci* 2009;12:996–1002.
7. Boiko T, Van Wart A, Caldwell JH, et al. Functional specialization of the axon initial segment by isoform-specific sodium channel targeting. *J Neurosci* 2003;23:2306–2313.
8. Hargus NJ, Merrick EC, Nigam A, et al. Temporal lobe epilepsy induces intrinsic alterations in Na channel gating in layer II medial entorhinal cortex neurons. *Neurobiol Dis* 2011;41:361–376.
9. Veeramah KR, O'Brien JE, Meisler MH, et al. De novo pathogenic SCN8A mutation identified by whole-genome sequencing of a family quartet affected by infantile epileptic encephalopathy and SUDEP. *Am J Hum Genet* 2012;90:502–510.
10. Blanchard MG, Willemsen MH, Walker JB, et al. De novo gain-of-function and loss-of-function mutations of SCN8A in patients with intellectual disabilities and epilepsy. *J Med Genet* 2015;52:330–337.
11. Estacion M, O'Brien JE, Conravey A, et al. A novel de novo mutation of SCN8A (Nav1.6) with enhanced channel activation in a child with epileptic encephalopathy. *Neurobiol Dis* 2014;69:117–123.
12. Wagnon JL, Korn MJ, Parent R, et al. Convulsive seizures and SUDEP in a mouse model of SCN8A epileptic encephalopathy. *Hum Mol Genet* 2015;24:506–515.
13. Boerma RS, Braun KP, van de Broek MPH, et al. Remarkable Phenytoin

Sensitivity in 4 Children with SCN8A-related Epilepsy: A Molecular Neuropharmacological Approach. *Neurotherapeutics* 2016;13:192-197.

14. Vaher U, Nõukas M, Nikopensius T, et al. De novo SCN8A mutation identified by whole-exome sequencing in a boy with neonatal epileptic encephalopathy, multiple congenital anomalies, and movement disorders. *J Child Neurol* 2014;29:202–206.
15. Herzog RI, Cummins TR, Ghassemi F, et al. Distinct repriming and closed-state inactivation kinetics of Nav1.6 and Nav1.7 sodium channels in mouse spinal sensory neurons. *JPhysiol* 2003;551:741-750.
16. Wagnon JL, Barker BS, Hounshell JA, et al. Pathogenic mechanism of recurrent mutations of SCN8A in epileptic encephalopathy. *Ann Clin Transl Neurol* 2015;doi.10.1002/acn3.276.
17. Remy S, Urban BW, Elger CE, et al. Anticonvulsant pharmacology of voltage-gated Na+ channels in hippocampal neurons of control and chronically epileptic rats. *EurJNeurosci* 2003;17:2648–2658.
18. Kuo CC, Bean BP. Slow binding of phenytoin to inactivated sodium channels in rat hippocampal neurons. *Mol Pharmacol* 1994;46:716–725.
19. Rogawski MA, Loscher W. The neurobiology of antiepileptic drugs. *Nat Rev Neurosci* 2004;5:553–564.
20. Singh R, Jayapal S, Goyal S, et al. Early-onset movement disorder and epileptic encephalopathy due to de novo dominant SCN8A mutation. *Seizure* 2015;26:69–71.
21. Smith MR, Goldin AL. Interaction between the sodium channel inactivation linker and domain III S4-S5. *Biophys J* 1997;73:1885–1895.
22. Ellerkmann RK, Remy S, Chen J, et al. Molecular and functional changes in voltage-dependent Na(+) channels following pilocarpine-induced status epilepticus in rat dentate granule cells. *Neuroscience* 2003;119:323–333.
23. Ketelaars SO, Gorter JA, van Vliet EA, et al. Sodium currents in isolated rat CA1 pyramidal and dentate granule neurones in the post-status epilepticus model of epilepsy. *Neuroscience* 2001;105:109–120.
24. Twombly DA, Yoshii M, Narahashi T. Mechanisms of calcium channel block by

phenytoin. *J Pharmacol Exp Ther* 1988;246:189–195.
25. Lenkowski PW, Batts TW, Smith MD, et al. A pharmacophore derived phenytoin analogue with increased affinity for slow inactivated sodium channels exhibits a desired anticonvulsant profile. *Neuropharmacology* 2007;52:1044–1054.
26. Macdonald RL, Kelly KM. Mechanisms of action of currently prescribed and newly developed antiepileptic drugs. *Epilepsia* 1994;35 Suppl 4:S41–50.
27. Hille B. Local anesthetics: hydrophilic and hydrophobic pathways for the drug-receptor reaction. *J Gen Physiol* 1977;69:497–515.

Figure Legends

Figure 1. I1327V modulates steady state activation. (A) Four-domain structure of the voltage-gated Na channel α subunit shows that I1327V is located at the cytosolic interface of the S4-S5 linker and transmembrane segment 5 of domain III. (B) Representative traces of families of Na currents recorded from ND7/23 cells transfected with the indicated $Na_v1.6$ cDNAs. (C) Averaged current-voltage (I-V) relationship for cells expressing WT and I1327V. Peak currents were normalized to cell capacitance. (D) Voltage dependence of channel activation. Smooth lines correspond to the least squares fit when average data were fit to a single Boltzmann equation. (E) Scatter plot of voltage at half-maximal activation ($V_{1/2}$) for cells expressing WT and I1327V. (F) Scatter plot of the slope factor of activation (k). (G) Average fast time constants obtained from single exponential fits to macroscopic current decays as a function of voltage. (H) Representative traces of normalized currents evoked by a +35 mV stimulus from a holding potential of -120 mV illustrate delays in macroscopic current decay between WT (black) and I1327V (red). Data are means ± S.E.M. Statistical significance: * $P < 0.05$; ** $P < 0.005$. Black circles, WT; red triangles, I1327V.

Figure 2. I1327V disrupts channel inactivation properties. (A) Average fast time constant obtained from single exponential fits to deactivation of WT and I1327V channels. (B) Voltage dependence of steady-state inactivation. Smooth lines correspond to the least squares fit when average data were fit to a single Boltzmann

equation. (C) Scatter plot of voltage at half-maximal inactivation ($V_{1/2}$) for cells expressing WT and I1327V (D) Scatter plot of the slope factor (k) of inactivation. (E) The window current is obtained by overlapping the normalized activation and inactivation curves from WT and I1327V cells. (F) Enhanced view of overlapping activation and inactivation curves shows an increase in I1327V window current (red shaded area) compared to WT (gray shaded area). G) Recovery from inactivation at a post train level of -90 mV. Data are means ± S.E.M. Statistical significance: * P <0.05; ** P<0.005. Black circles, WT; red triangles, I1327V.

Figure 3. Phenytoin (PHT) inhibits Na channel currents evoked from WT and I1327V and modulates steady-state activation parameters. (A) Scatter plot showing normalized macroscopic current amplitude remaining following tonic block by phenytoin (100 μM). Currents were elicited by a depolarizing step to 0 mV for 12 ms from a holding potential of -60 mV. (B) Representative traces show greater tonic inhibition of I1327V currents over WT currents by phenytoin (100 μM) (C) Use-dependent block by phenytoin (100 μM). Cells were held at -120 mV and a voltage step to +20 mV was applied for 20 ms at a frequency of 10 Hz. (D) Shift in the voltage dependence of WT channel activation following treatment with phenytoin (100 μM). Smooth lines correspond to the least squares fit when average data were fit to a single Boltzmann equation. (E) Scatter plot of voltage at half-maximal activation ($V_{1/2}$) (F) Shift in the voltage dependence of I1327V channel activation following treatment with phenytoin (100 μM). Smooth lines correspond to the least squares fit when average data were fit to a single Boltzmann equation. (G) Scatter plot of voltage at half-maximal activation ($V_{1/2}$). Data are means ± S.E.M. Statistical significance: *P <0.05. Black filled circles, WT; blue open circles, WT + phenytoin, red filled triangles, I1327V; orange open triangles, I1327V + phenytoin.

Figure 4. Phenytoin (PHT) modulates steady state inactivation properties in cells expressing WT and I1327V channels. (A) Shift in the voltage dependence of WT channel inactivation following treatment with phenytoin (100 μM). Smooth lines correspond to the least squares fit when average data were fit to a single Boltzmann equation. (B) Scatter plot of voltage at half-maximal inactivation ($V_{1/2}$). (C)

Representative WT traces elicited following a pre-pulse to -75 mV demonstrating the shift in inactivation following application of phenytoin (100 μM). Traces were normalized to the pre-phenytoin peak current. (D) Shift in the voltage dependence of I1327V channel inactivation following treatment with phenytoin (100 μM). Smooth lines correspond to the least squares fit when average data were fit to a single Boltzmann equation. (E) Scatter plot of voltage at half-maximal inactivation ($V_{1/2}$). (F) Representative I1327V traces following a pre-pulse to -75 mV demonstrating the shift in inactivation following the application of phenytoin (100 μM). Recovery from inactivation before and after the application of phenytoin (100 μM) in WT (G) and I1327V (H) cells. Data are means ± S.E.M. Statistical significance *P <0.05; **P<0.005. Black filled circles, WT; blue open circles, WT + phenytoin; red filled triangles, I1327V; orange open triangles, I1327V + phenytoin.

epi_13461_first_author_photo_(300_dpi).jpg

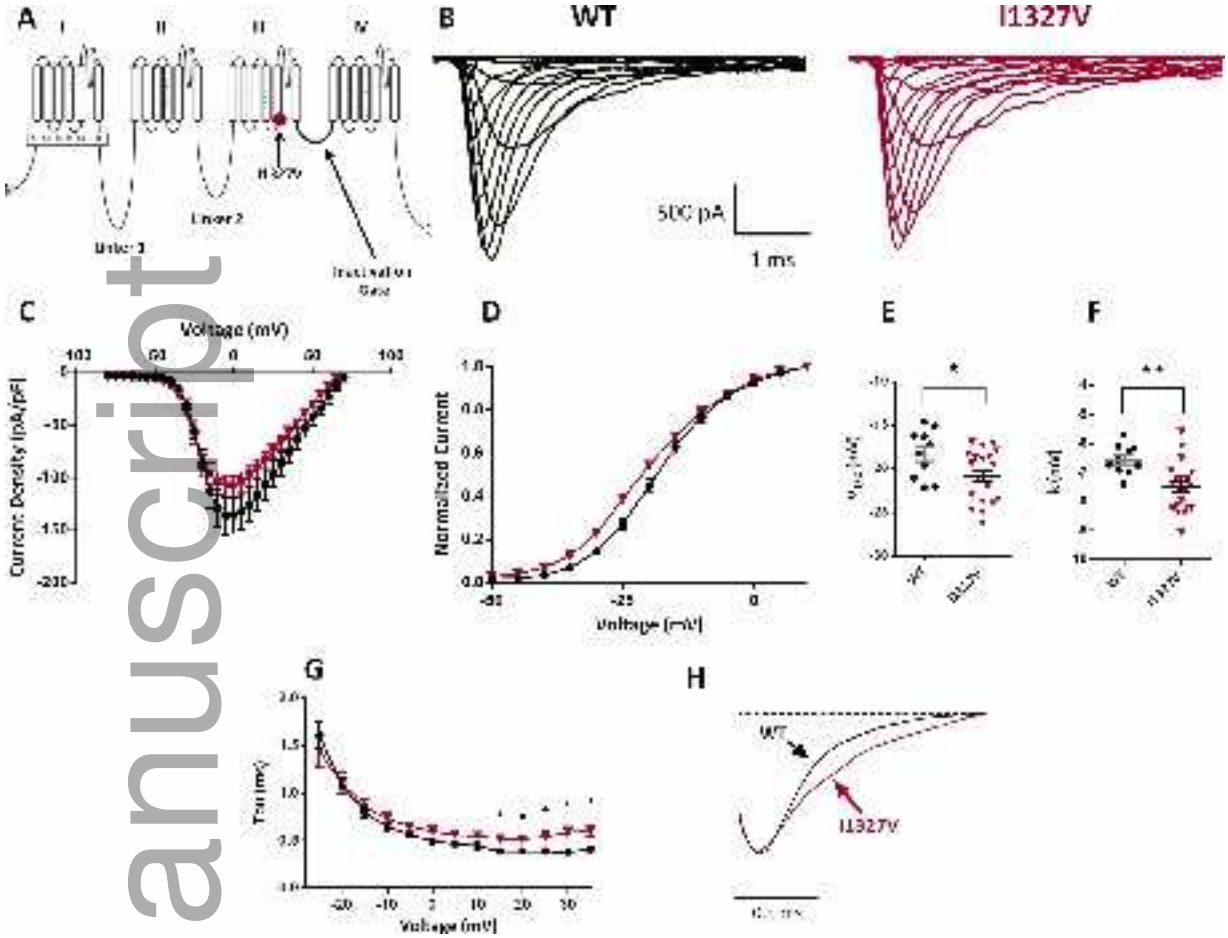

epi_13461_f1.tif

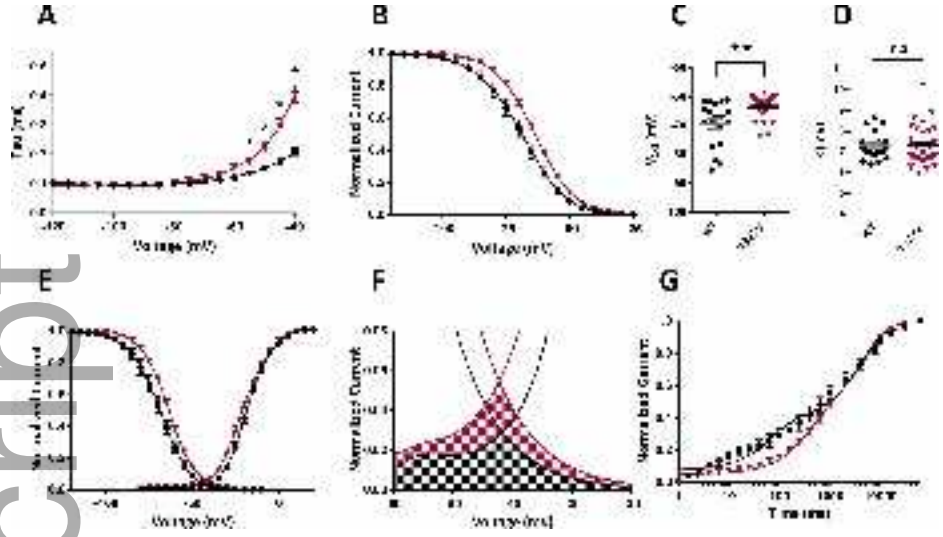

epi_13461_f2.tif

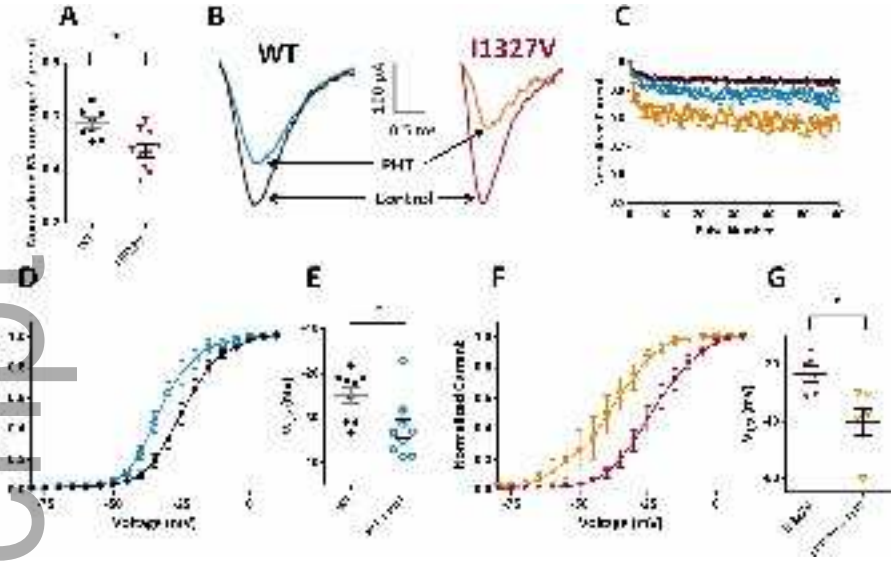

epi_13461_f3.tif

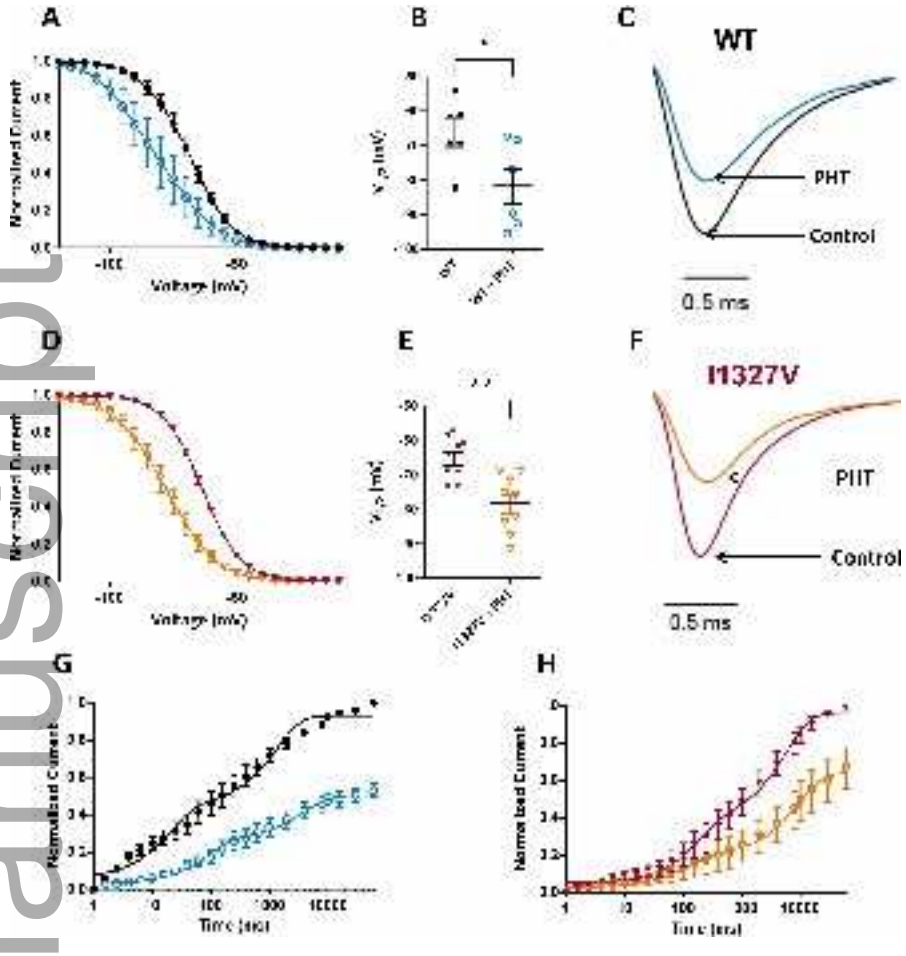

epi_13461_f4.tif